

See discussions, stats, and author profiles for this publication at: <https://www.researchgate.net/publication/334168163>

# Photonic Network-on-Chip (NoC) Architectures for the High Performance Computing Systems

Conference Paper · December 2018

DOI: 10.1109/ASPCON.2018.8748654

CITATIONS

0

READS

26

2 authors, including:



[Sayani Sarkar](#)

Bellarmino University

11 PUBLICATIONS 46 CITATIONS

SEE PROFILE

Some of the authors of this publication are also working on these related projects:



Intelligent Drone based Surveillance [View project](#)

# Photonic Network-on-Chip (NoC) Architectures for the High Performance Computing Systems

Sayani Sarkar

*School of Computing and Informatics  
Ray P. Authement College of Sciences  
University of Louisiana at Lafayette  
301 E. Lewis Street, Lafayette, LA 70503  
e-mail: c00270565@louisiana.edu*

Shantanu Pal

*Sigtuple Technologies Private Limited  
Bangalore 560102, India  
e-mail: shantanu.pal@hotmail.com*

**Abstract**—Higher memory-bandwidth requirement in multi-core computing systems to comply with memory requests from large number of cores can be suitably addressed by replacing traditional electrical network-on-chips (ENoCs) with photonic network-on-chips (PNoCs). Further, energy efficiency of these systems can be significantly improved by replacing electronic on-chip interconnects with silicon nanophotonic interconnects which have higher bandwidth and lower latency. However, the ultimate performance of these systems is limited by the static power for laser sources and waveguide propagation losses. LumiNOC is a nanophotonic network-on-chip (PNoC) architecture, which partitions the entire network into multiple subnetworks for better efficiency. It also uses a distributed arbitration scheme and a channel sharing mechanism for data transmission. Laser sources and ring resonators used in this configuration are expected to have matched optical frequencies for reliable operation. But, thermal sensitivity of photonic devices and process parameters variations inherent during manufacturing process always results in frequency mismatch. An adaptive frequency tuning technique can be used to reduce the difference in resonant frequencies among ring resonators, reduce frequency differences for corresponding on-chip lasers and ultimately to reduce the thermal tuning power of LumiNOC structures.

**Index Terms**—Multiprocessor inter-connection networks, nanophotonics, silicon photonics, optical interconnects, ring resonator, optical tuning, thermal management.

## I. INTRODUCTION

Ever-increasing need for higher memory-bandwidth in multi-core systems to support their thread-level parallelism can be adequately addressed by replacing traditional electrical network-on-chips (ENoCs) with photonic network-on-chips (PNoCs). Also energy efficiency of these systems can be further improved by replacing electrical on-chip interconnects with photonic interconnects [1]. Silicon nanophotonic chips which typically include laser source, ring modulator, filter, passive waveguide and a photodetector can be used to meet the higher bandwidth requirement of next-generation multi-core systems and also to establish low-power communication links over extended distances. It is essential that the frequency of the laser source powering a photonic-chip should match with resonant frequencies of on-chip ring modulators and filters for efficient operation. In photonic network-on-chips, ring resonators are in general placed closer to cores for reducing the delay and energy consumption of electrical links connecting

cores with transmitters and receivers. Resonant frequencies of ring resonators are very much sensitive to any variation in device temperature and various fabrication parameters. Consequently, any change in fabrication process parameters or core power consumption can alter the temperature of ring resonators and thereby introduce data transmission errors. Thermal tuning via micro-heaters [2] can be used to match the resonant frequencies of ring resonators and also frequencies of laser sources in photonic network-on-chips (PNoC). The use of on-chip laser sources in PNoC structures can also reduce the thermal tuning power required due to their close proximity to control circuits [3]. An adaptive frequency tuning technique can be used in LumiNOC structures to simultaneously match optical frequencies of both on-chip laser sources and ring resonators resulting in overall reduction of the tuning power. In multi-core systems workload can be suitably distributed among various cores to achieve an acceptable on-die temperature gradient that can minimize the difference among resonant frequencies of on-chip ring resonators and laser sources. Subsequently, any remaining difference in their frequencies can be compensated by local thermal tuning.

## II. PHOTONIC NETWORK-ON-CHIP : LUMINOC ARCHITECTURE

LumiNOC is a novel photonic network-on-chip (PNoC) architecture which has higher memory-bandwidth, lower latency and it is more energy-efficient in nature compared with conventional network-on-chip architectures. In this structure, the entire network is broken into multiple sub-networks of smaller lengths to reduce the power consumption. Figure 1 shows the schematic of a 16-node chip multiprocessor system that has been developed using LumiNOC architecture with different sub-network designs [4]. In this structure, all tiles are interconnected with the help of one horizontal and one vertical sub-network. To minimize the transmission delay both sender and receiver ring-resonators are co-located within the same sub-network. Same wavelength is used for both channel arbitration and parallel data transmission to use the hardware efficiently and it also reduces the overall power consumption. Multiple tiles are connected to a single channel to improve the channel utilization. Limited number of channels are used in an

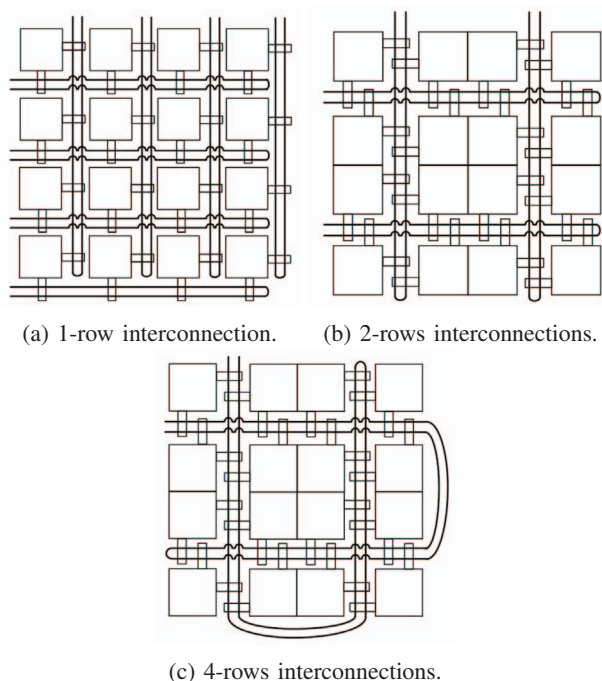


Fig. 1. 16-tiles chip multiprocessor with LumiNOC interconnections [4].

interconnect and multiple waveguides are used in every sub-network to improve the power efficiency of the system. Figure 2 shows the schematic of a one-row sub-network structure with shared channel configuration. In this structure, each tile

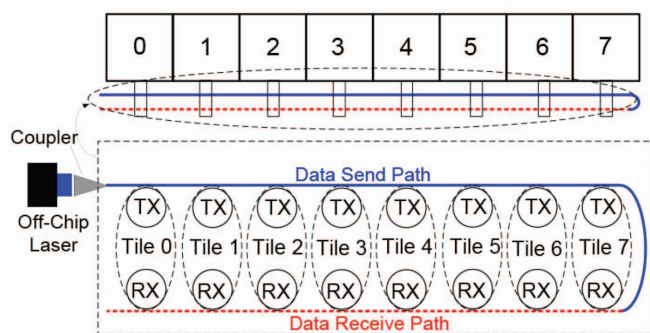


Fig. 2. Sub-network structure in LumiNOC configuration with eight nodes ( $T_X$  - transmitter ring resonator,  $R_X$  - receiver ring resonator) [4].

contains one transmitter ( $T_X$ )-ring (for signal modulation) and one receiver( $R_X$ )-ring (for signal receiving). When the signal propagates through the waveguide, transmitter ( $T_X$ )-rings of various nodes in the signal path (solid line) are connected in series. The signal to be transmitted, is modulated by one of the transmitter-ring (at any of the nodes) and it can be received by receiver-rings available at any other nodes including the node modulating the signal. During the data transmission, a particular modulator-ring modulates all signal wavelengths, whereas receivers are tuned to receive all wavelengths. During

the signal transmission phase, the access of photonic channels shared by optical signals is coordinated by an optical collision detection and dynamic channel scheduling mechanism. Before the data transmission starts, a dynamic and fair scheduling for the channel acquisition is carried out based on the index of the node sending the data and a global cycle count. To do this, each sender transmits an abbreviated version of arbitration flags (destination address and packet size). Once the flag is received by all nodes, the data transmission starts with a single sender and receiver for the duration of the packet (based on the arbitration flag received). Upon completion of the data transfer process by the first transmitter, similar process is repeated for the next transmitter and so on. The channel remains occupied until the transmission process is completed. Once the transmission phase is over, the channel goes idle and a new arbitration process is started to acquire the channel one again and the process is continued in this way.

### III. ADAPTIVE TUNING OF LUMINOC STRUCTURE

Energy-efficient, densely integrated photonic platforms have been developed for signal generation and reception following recent advances in low-loss silicon nano-photonics technology and integration of the same with commercial CMOS chip manufacturing processes. Electronic drivers has been kept in very close-proximity with photonic components in a single chip using monolithic CMOS platform integration. In LumiNoC architectures fabricated using silicon photonic technology ring resonators could be placed closer to processor cores to reduce the time-delay and energy consumption by the electrical links connecting cores to photonic link transmitter and receiver. A change in temperature of ring resonators due to variation in core power consumption can result in data transmission errors. Thermal tuning using on-chip micro-heaters [2] is the most commonly used technique to compensate for the frequency difference. An intelligent workload allocation policy along with local temperature tuning of ring resonators can be used to match resonant frequencies of on-chip ring resonators with frequencies of laser sources. In a LumiNoC structure, the electrical power necessary to control and tune the optical frequency of on-chip devices is dependent on various parameters, e.g. workload distribution, device thermal state and process parameters variation as shown in Figure 3. Once an application

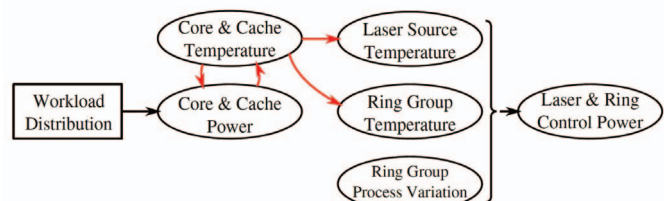


Fig. 3. Dependence of various parameters (workload distribution, device thermal state, process parameters variation) on the electrical power necessary for controlling resonant frequency of on-chip ring resonators in LumiNoC [5].

with multiple threads arrives, before starting of the system operation they are initially assigned to different cores so as to balance resonant frequencies of various ring groups. Then resonant frequencies for various ring groups are estimated and the process is iterated multiple times until the assignment has been completed for all threads. Intelligent workload allocation can be used to decrease the difference in resonant frequencies among various groups of ring resonators. Silicon micro-ring resonators which are one of the key elements in optical networks-on-chips [6] have a sharp dependence of their resonance condition on various fabrication-induced imperfections and any deviations from designed parameters can severely degrade their performance. Hence, it is critical to develop an on-chip adaptive feedback-based tuning method to actively monitor and tune optical performances for silicon ring-resonator based devices and subsequently lock their frequencies for spectral alignment in real time for a large number of interconnected devices. Figure 4 shows the schematic of a

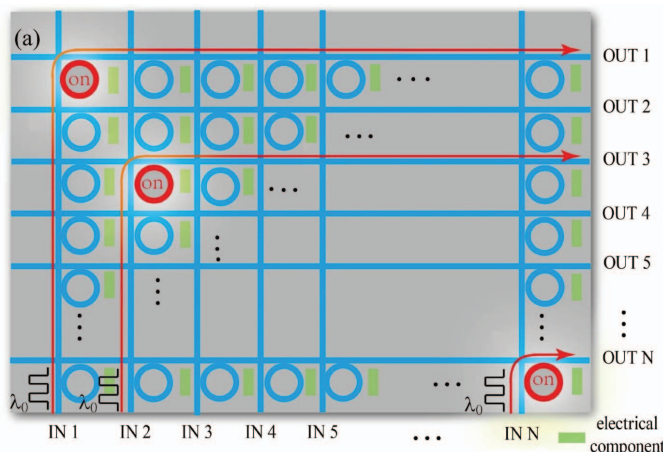


Fig. 4. Schematic of a  $N \times N$  MIMO switch-matrix array developed using adaptively tuned silicon ring-resonator as a switch element. Ring-resonators (in on-state) and optical links have been shown in red color. [7]

silicon ring-resonator based on-chip optical router with multiple input and multiple output ports (MIMO) [7], [8]. Here,  $\lambda_0$  represents the wavelength of a communication channel. In this structure, switch elements in the off-state i.e. ring-resonators with their resonance wavelengths detuned from  $\lambda_0$ , direct  $\lambda_0$  through throughput-ports. On the other hand, switch elements in the on-state i.e. ring-resonators with their resonance wavelengths tuned to  $\lambda_0$ , direct  $\lambda_0$  to drop-ports. Hence, signals from a given input-port are routed to an output-port through switching-on only one ring-resonator (switch), while all other ring-resonators in the link remain in the off-state. Figure 5 shows the schematic of an optical switch developed using a silicon ring-resonator coupled with a waveguide crossing. In this structure, each ring-resonator is integrated with two electrically isolated lateral p-i-n diodes and one micro-heater (for adaptive tuning). p<sup>-</sup>-doped wires have been introduced between two diodes for blocking carrier leakage and to mini-

mize the leakage current. Here, the diode with ion-implanted intrinsic region under reverse-bias condition serves as a defect-state-absorption (DSA)-based photo-current monitor for the ring-resonator internal power, while the other diode serves as an electro-optic tuner (switch) under forward-bias condition. Figure 6 shows both transmission and photo-current spectra

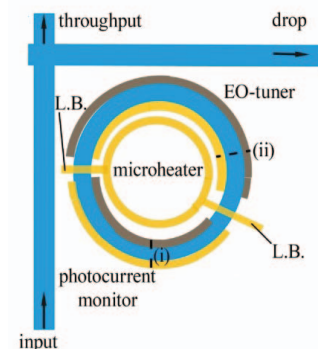
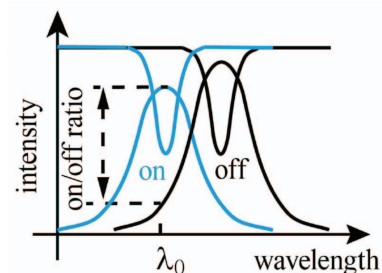
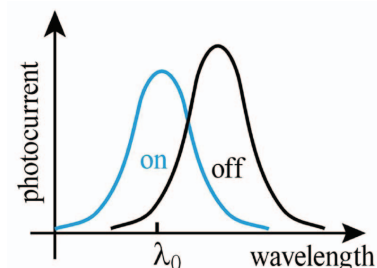


Fig. 5. Silicon ring-resonator coupled with a waveguide crossing (Optical switch) and on-chip micro-heater for adaptive tuning. [7]

of an optical switch at both on- and off-states. Here, signals



(a) Transmission spectra of an optical switch (schematic). [7]



(b) Photo-current spectra of an optical switch (schematic). [7]

Fig. 6. Responses of an optical switch in both on- and off-states. [7]

from an input-port of the optical switch can be routed to the output-port only by switching-on only one switch element, while all other ring-resonators along the link remain at an off-state. The optical switch remains in the off-state without applying a bias voltage, whereas it remains in the on-state upon forward-biasing the switch. The photocurrent spectra



follows the resonance line-shape of both ring-resonator cavity internal and drop-port transmission spectra and hence it can be used as a monitoring signal [9]. Figure 7 shows the typical

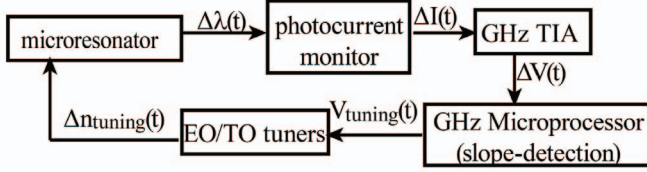


Fig. 7. Control scheme for adaptive tuning (schematic) under closed-loop condition. [7]

control scheme (schematic) of the adaptive tuning process under closed-loop conditions for a ring-resonator. The spectral misalignment ( $\Delta\lambda(t)$ ) between the ring-resonator resonance wavelength and the carrier wavelength at a given time  $t$  is due to the drop ( $\Delta I(t)$ ) in the time-averaged sampled photocurrent  $I(t)$  generated inside a ring-resonator. The amplified value of  $\Delta I(t)$  can be used as an input voltage  $\Delta V(t)$  to a microprocessor, which can be used as a feedback voltage to control the output voltage ( $V_{tuning}(t)$ ) of the integrated electro-optic/thermo-optic tuner. This feedback voltage can be used to compensate for the spectral misalignment of the ring-resonator with an adaptive tuning ( $\Delta n_{tuning}(t)$ ) in the refractive index of the ring-resonator. Figure 8 shows three

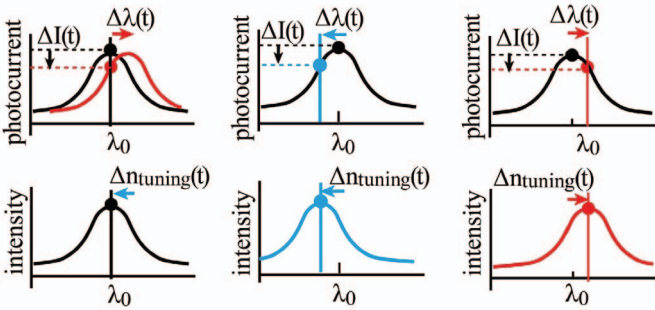


Fig. 8. Resonance wavelength of the ring-resonator as a function of temperature. [7]

different cases of the change in sampled photo-current and resulting adaptive tuning in the resonant wavelength of the ring-resonator. There can be either red-shift ( $+\Delta\lambda$ ) or blue-shift ( $-\Delta\lambda$ ) in the resonance wavelength ( $\lambda_0$ ) due to on-chip temperature rise or fall respectively. The middle and right columns show the cases that the carrier wavelength is blue- and red-drifted from the resonant wavelength. For a red-shift (blue-shift) in the resonance wavelength, the electro-optic (EO) tuner blue-shifts (red-shifts) the resonance wavelength to preserve the spectral alignment at the carrier wavelength  $\lambda_0$ . For a red-drift in the carrier wavelength, the thermo-optic (TO) tuner red-shifts the resonance wavelength to preserve the spectral alignment at the new (red-drifted) carrier wavelength. Hence, the change in the carrier wavelength ( $\Delta\lambda(t)$ ) can be written

as follows:

$$\Delta\lambda(t) = \lambda_{res}(t) - \lambda_{carrier}(t) + \Delta\lambda_{tuning}(t) \quad (1)$$

Here,  $\lambda_{res}(t)$  is the resonance wavelength,  $\lambda_{carrier}(t)$  is the carrier wavelength and  $\Delta\lambda_{tuning}(t)$  is the change in resonance wavelength due to the change in the refractive index ( $\Delta n_{tuning}(t)$ ) of the ring-resonator. The variation in  $\lambda_{res}(t)$  due to on-chip temperature variation ( $\Delta T(t)$ ) can be written as follows:

$$\lambda_{res}(t) = \lambda_0(t) + \left(\frac{d\lambda}{dT}\right) \cdot \Delta T(t) \quad (2)$$

and

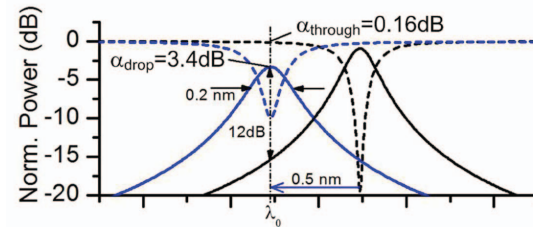
$$\frac{d\lambda}{dT} = \left(\frac{\lambda_0}{n_g}\right) \cdot \left(\frac{dn}{dT}\right) \quad (3)$$

Here,  $n_g$  is the group refractive index of the silicon waveguide and  $(dn/dT)$  is the TO-coefficient for silicon. For a continuous drift in the carrier wavelength (i.e. for  $\lambda_{carrier}(t) = \lambda_0 + \Delta\lambda_{carrier}(t)$ ), it is possible to write  $\lambda_{tuning}(t) = (\lambda_0/n_g) \cdot \Delta n_{tuning}(t)$ . Hence,  $\Delta\lambda(t)$  can be re-written using equations 1 and 2 as follows:

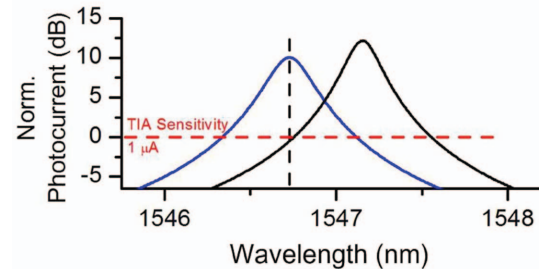
$$\Delta\lambda(t) = \left(\frac{d\lambda}{dT}\right) \cdot \Delta T - \Delta\lambda_{carrier}(t) + \left(\frac{\lambda_0}{n_g}\right) \cdot \Delta n_{tuning}(t) \quad (4)$$

For preserving the spectral alignment,  $\Delta\lambda(t)$  should be always very close to zero during the monitoring and adaptive tuning processes.

Figure 9a shows the calculated optical transmission spectra of



(a) Optical transmission spectra (calculated) of a ring-resonator : off-state throughput-port - black dashed line, off-state drop-port : black solid-line, on-state throughput-port - blue dashed line and on-state drop-port - blue solid line.



(b) Photo-current spectra (calculated) of the ring-resonator : off-state - black solid-line, on-state - blue solid-line. [10]

Fig. 9. Optical transmission and photo-current spectra of a ring-resonator.

the switch element (ring-resonator) in both on- and off- state at

1550 nm. Figure 9b shows the calculated photo-current spectra for  $P_0 = 100 \mu\text{W}$ . While using the photo-current as a feedback signal to the microprocessor for a closed-loop and controlled tuning of the resonance wavelength, at first the photo-current is sampled for a time -  $\tau_{\text{sampling}}$  and then the spectral misalignment is extracted based on a slope-detection method. The type of the tuner to be used and the amount of tuning needed within a period of time  $\tau_{\text{tuning}}$  is determined. Total processing time -  $\tau_{\text{proc}}$  and tuning time -  $\tau_{\text{tuning}}$  defines the active period  $\tau_{\text{active}}$  within each loop of the microprocessor. The slope-detection method has been schematically explained in the Figure 10. Initially, the microprocessor samples a photo-

current as follows:

$$\Delta n_{\text{tuning}}(t) = \left( \frac{dn}{dT} \right) \cdot \Delta T_{\text{tuning}}(t) \left( \frac{L_{T0}}{L_{\text{tot}}} \right) \quad (5)$$

where  $L_{T0}$  is the length of the ring-resonator under thermo-optic tuning and  $\Delta n_{\text{tuning}}(t)$  is change in refractive index of the ring-resonator as obtained by the thermo-optic tuning. In general,  $L_{T0} \approx L_{\text{tot}}$  as the entire ring-resonator is heated up due to thermal diffusion from the micro-heater towards inner radius of the ring-resonator. Since silicon has a relatively large TO-coefficient, the final  $\Delta n_{\text{tuning}}(t)$  that can be obtained by TO-tuning is practically limited by the temperature rise that is imposed on the ring-resonator.

#### IV. CONCLUSIONS

Photonic network-on-chips are a promising replacement of electrical network-on-chip in next generation multi-core processors for energy-efficient and higher bandwidth operation. Inefficiencies in these architectures are mainly caused by channel over-provisioning, optical losses due to topology and photonic devices layout, power overhead from separated arbitration channels and networks and also due to the heating effect. These issues can be addressed in LumiNoC structure by adopting a shared-channel, photonic on-chip network with a novel, in-band arbitration mechanism to efficiently utilize the power, thereby achieving a high performance, and scalable interconnect with extremely low latency. In addition to that an use of thermal tuning and adaptive tuning method can additionally compensate for the performance mismatch during wide-band operation and can also reduce the local thermal tuning power. Hence, LumiNoc architecture with adaptive tuning has the potential to achieve a lower latency with higher throughput per Watt even under a considerable traffic load.

#### REFERENCES

- [1] S. Abadal, M. Iannazzo, M. Nemirovsky, A. Cabellos-Aparicio, H. Lee, and E. Alarcn, "On the Area and Energy Scalability of Wireless Network-on-Chip: A Model-Based Benchmarked Design Space Exploration," *IEEE/ACM Transactions on Networking*, vol. 23, no. 5, pp. 1501–1513, Oct 2015.
- [2] C. T. DeRose, M. R. Watts, D. C. Trotter, D. L. Luck, G. N. Nielson, and R. W. Young, "Silicon microring modulator with integrated heater and temperature sensor for thermal control," in *CLEO/QELS: 2010 Laser Science to Photonic Applications*, San Jose, CA, USA, 5 2010, pp. 1–2.
- [3] M. J. R. Heck and J. E. Bowers, "Energy Efficient and Energy Proportional Optical Interconnects for Multi-Core Processors: Driving the Need for On-Chip Sources," *IEEE Journal of Selected Topics in Quantum Electronics*, vol. 20, no. 4, pp. 332–343, July 2014.
- [4] C. Li, M. Browning, P. V. Gratz, and S. Palermo, "LumiNOC: A Power-Efficient, High-Performance, Photonic Network-on-Chip," *IEEE Transactions on Computer-Aided Design of Integrated Circuits and Systems*, vol. 33, no. 6, pp. 826–838, 2014.
- [5] J. L. Abelln, A. K. Coskun, A. Gu, W. Jin, A. Joshi, A. B. Kahng, J. Klamkin, C. Morales, J. Recchio, V. Srinivas, and T. Zhang, "Adaptive Tuning of Photonic Devices in a Photonic NoC Through Dynamic Workload Allocation," *IEEE Transactions on Computer-Aided Design of Integrated Circuits and Systems*, vol. 36, no. 5, pp. 801–814, 2017.
- [6] W. Bogaerts, P. D. Heyn, T. V. Vaerenbergh, K. D. Vos, S. K. Selvaraja, T. Claes, P. Dumon, P. Bienstman, D. V. Thourhout, and R. Baets, "Silicon microring resonators," *Laser & Photonics Reviews*, vol. 6, no. 1, pp. 47–73, 2011.

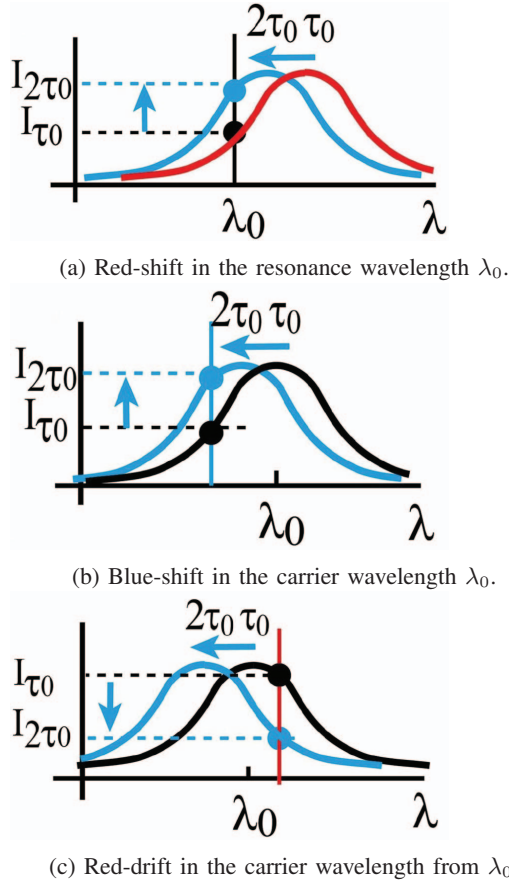


Fig. 10. Slope-detection method for adaptive tuning [7].

current  $I_{\tau_0}$  at time  $\tau_0$ , then it carries out the second sampling of the photo-current  $I_{2\tau_0}$  at time  $2\tau_0$  upon the blue-shifted resonance (assuming  $\tau_0 < 10 \text{ ns}$ ). When the resonance is red-detuned (as shown in Figure 10a), a blueshift results in  $I_{2\tau_0} > I_{\tau_0}$  (Figure 10b). When the resonance is blue-detuned, the blue-shift results in  $I_{2\tau_0} < I_{\tau_0}$  (as shown in Figure 10c). Therefore, this allows the microprocessor to determine within  $\tau_{\text{proc}}$  the type of tuning and the tuning voltage needed based on the value of  $I_{\tau_0}$ . For a carrier wavelength red-drift, the change in refractive index ( $\Delta n_{\text{tuning}}(t)$ ) needed to red-shift the resonance wavelength thermo-optically can be written as

- [7] Y. Zhang, Y. Li, S. Feng, and A. W. Poon, "Towards adaptively tuned silicon microring resonators for optical networks-on-chip applications," *IEEE Journal of Selected Topics in Quantum Electronics*, vol. 20, no. 4, pp. 136–149, jul 2014.
- [8] S. Fathpour, K. K. Tsia, and B. Jalali, "Two-photon photovoltaic effect in silicon," *IEEE Journal of Quantum Electronics*, vol. 43, no. 12, pp. 1211–1217, dec 2007.
- [9] Y. Li, S. Feng, Y. Zhang, and A. W. Poon, "In-microresonator linearabsorption-based real-time photocurrent-monitoring and tuning with closed-loop control for silicon microresonators," Patent U.S. Patent 14/057,679, 2013.
- [10] M. Georgas, J. Orcutt, R. J. Ram, and V. Stojanovic, "A monolithically-integrated optical receiver in standard 45-nm SOI," in *2011 Proceedings of the ESSCIRC (ESSCIRC)*. Helsinki, Finland: IEEE, 2011.